Multimodel Ensemble Sea Level Forecasts for Tropical Pacific Islands

MATTHEW J. WIDLANSKY,[a,b] JOHN J. MARRA,[c] MD. RASHED CHOWDHURY,[d] SCOTT A. STEPHENS,[e] ELAINE R. MILES,[f] NICOLAS FAUCHEREAU,[e] CLAIRE M. SPILLMAN,[f] GRANT SMITH,[f] GRANT BEARD,[f] AND JUDITH WELLS[a]

[a] *Joint Institute for Marine and Atmospheric Research, School of Ocean and Earth Science and Technology, University of Hawai'i at Mānoa, Honolulu, Hawaii*
[b] *International Pacific Research Center, School of Ocean and Earth Science and Technology, University of Hawai'i at Mānoa, Honolulu, Hawaii*
[c] *NOAA/NESDIS/National Centers for Environmental Information, Inouye Regional Center, Honolulu, Hawaii*
[d] *Pacific ENSO Applications Climate Center, Joint Institute for Marine and Atmospheric Research, University of Hawai'i at Mānoa, Honolulu, Hawaii*
[e] *National Institute of Water and Atmospheric Research, Hamilton, New Zealand*
[f] *Bureau of Meteorology, Melbourne, Victoria, Australia*

(Manuscript received 22 August 2016, in final form 15 November 2016)

ABSTRACT

Sea level anomaly extremes impact tropical Pacific Ocean islands, often with too little warning to mitigate risks. With El Niño, such as the strong 2015/16 event, comes weaker trade winds and mean sea level drops exceeding 30 cm in the western Pacific that expose shallow-water ecosystems at low tides. Nearly opposite climate conditions accompany La Niña events, which cause sea level high stands (10–20 cm) and result in more frequent tide- and storm-related inundations that threaten coastlines. In the past, these effects have been exacerbated by decadal sea level variability, as well as continuing global sea level rise. Climate models, which are increasingly better able to simulate past and future evolutions of phenomena responsible for these extremes (i.e., El Niño–Southern Oscillation, Pacific decadal oscillation, and greenhouse warming), are also able to describe, or even directly simulate, associated sea level fluctuations. By compiling monthly sea level anomaly predictions from multiple statistical and dynamical (coupled ocean–atmosphere) models, which are typically skillful out to at least six months in the tropical Pacific, improved future outlooks are achieved. From this multimodel ensemble comes forecasts that are less prone to individual model errors and also uncertainty measurements achieved by comparing retrospective forecasts with the observed sea level. This framework delivers online a new real-time forecasting product of monthly mean sea level anomalies and will provide to the Pacific island community information that can be used to reduce impacts associated with sea level extremes.

1. Introduction

Tropical Pacific Ocean islands experience large interannual variations of sea level (Figs. 1a and 2) with occasionally severe coastal impacts such as prolonged inundations (high-water stands) or exposures (low-water stands) over many tidal cycles. Sea level variations operate across the Pacific and are a well-known aspect of El Niño–Southern Oscillation (ENSO) (e.g., Merrifield et al. 1999; Wyrtki 1984). During past strong El Niño events (e.g., 1982/83 and 1997/98), sea levels have been observed to drop by more than 30 cm around tropical western Pacific islands (Becker et al. 2012) relative to the long-term climatology (Fig. 2), potentially damaging coral reefs and associated coastal ecosystems (Widlansky et al. 2014). Conversely, during La Niña events, above-normal sea levels up to 20 cm higher (Chowdhury et al. 2007) increase the risks of damage to infrastructure and salinization of aquifers from coastal inundations caused by waves or storm surges (Becker et al. 2014), compounding the effects of gradual sea level rise due to climate change.

Whereas ENSO prediction has matured over the past several decades (Jin et al. 2008; McPhaden et al. 2015) to include sophisticated multimodel ensemble forecasts of upcoming seasons (Barnston et al. 2015), predictions of

Corresponding author e-mail: Matthew J. Widlansky, mwidlans@hawaii.edu

DOI: 10.1175/JAMC-D-16-0284.1

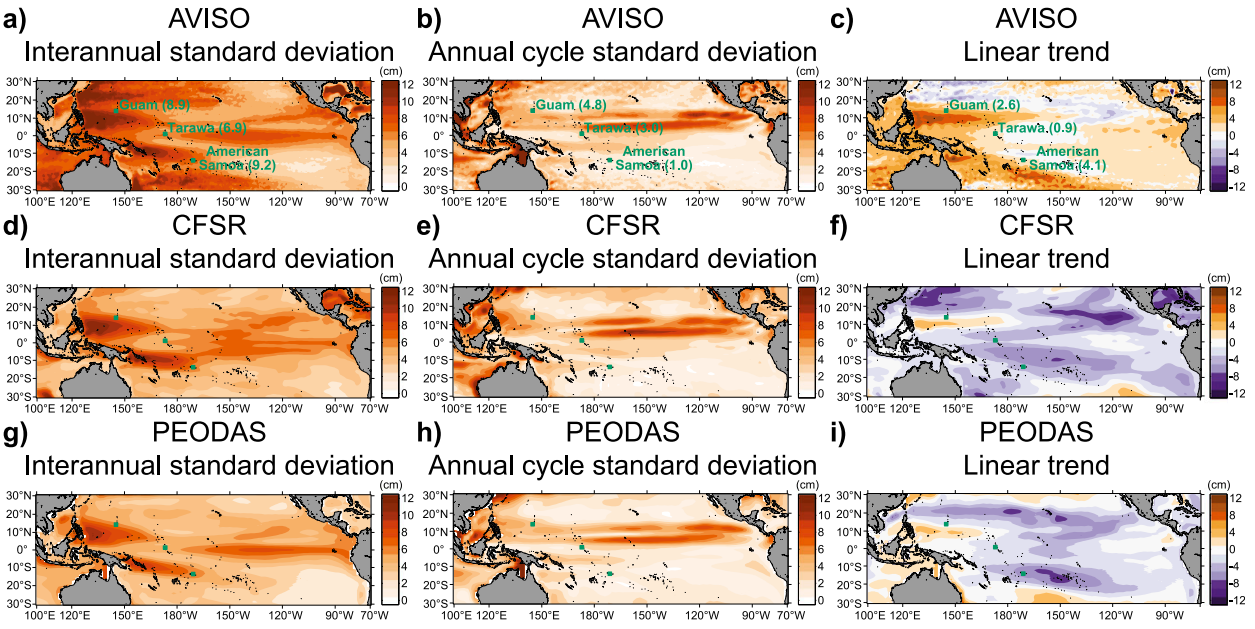

FIG. 1. Sea surface height variability (cm) as (a)–(c) observed from monthly mean AVISO satellite altimetry and island tide gauges (shading and numbers, respectively) and simulated by climate-model reanalyses [(d)–(f) CFSR and (g)–(i) PEODAS] on (left) interannual, (center) annual-cycle, and (right) decadal time scales. The first two columns show the standard deviation of anomalies (during 1993–2014) and climatology (1999–2010 average). In the right column, the linear trend (1999–2013) includes decadal variability as well as long-term global sea level rise, which is not well resolved by the reanalyses. The boxes (2° latitude × 2° longitude) and labels represent the island averaging regions used throughout the paper.

monthly and seasonal sea level variability are limited to only a few statistical (Chowdhury and Chu 2015; Chowdhury et al. 2014) or dynamical (McIntosh et al. 2015; Miles et al. 2014) models, which are typically considered individually. Merging such sea level predictions into a multimodel monthly sea level anomaly forecast ensemble should, in principle, yield a more comprehensive representation of uncertainty (i.e., forecasts would be less sensitive to individual model errors and thus be more accurate).

Besides providing more accurate predictions of monthly sea level anomalies, an improved seasonal sea level forecast product should also integrate with existing sea level outlooks for other time frames (e.g., tide predictions or sea level rise projections). For the tropical Pacific, island communities are particularly vulnerable to future incremental increases in absolute sea level and its potential threat to infrastructure (Keener et al. 2012). These increases are often dominated by global changes (e.g., sea level rise) that are not yet resolved by seasonal prediction models but that we can estimate from observations (Church and White 2011; Merrifield et al. 2012) or future climate projections (Church et al. 2013). To address more immediate risks, stakeholders also desire a forecast conveying more frequent relative changes (i.e., monthly rising or falling sea levels) caused by climate variability such as ENSO. Furthermore, astronomical tides—for which well-established predictions are used widely—typically exert the largest control on hourly to daily coastal sea levels in the tropical Pacific, as is common globally. Clearly, a complete sea level forecast must incorporate all of these influences on the sea level (i.e., long-term trends, monthly variability, and tides) into a prediction product.

Here we describe a new initiative to produce multimodel monthly sea level anomaly forecasts out to six months that can be used to generate coastal sea level alerts. We use recent advances to better resolve the observed sea level, required to initialize and verify statistical models, and to simulate interannual sea level variability in the tropical Pacific using global climate models (Landerer et al. 2014; Roberts et al. 2016). Our forecast ensemble includes three statistical models, capturing how sea level varies as a function of sea surface temperature (SST) and two dynamical models of the coupled ocean–atmosphere climate. To assess the multimodel performance, we conducted retrospective forecasts (1979–2014) of sea level anomalies around three islands, sampling a wide swath of the tropical western and central Pacific (Guam, Tarawa, and American Samoa; labeled in Fig. 1), which were

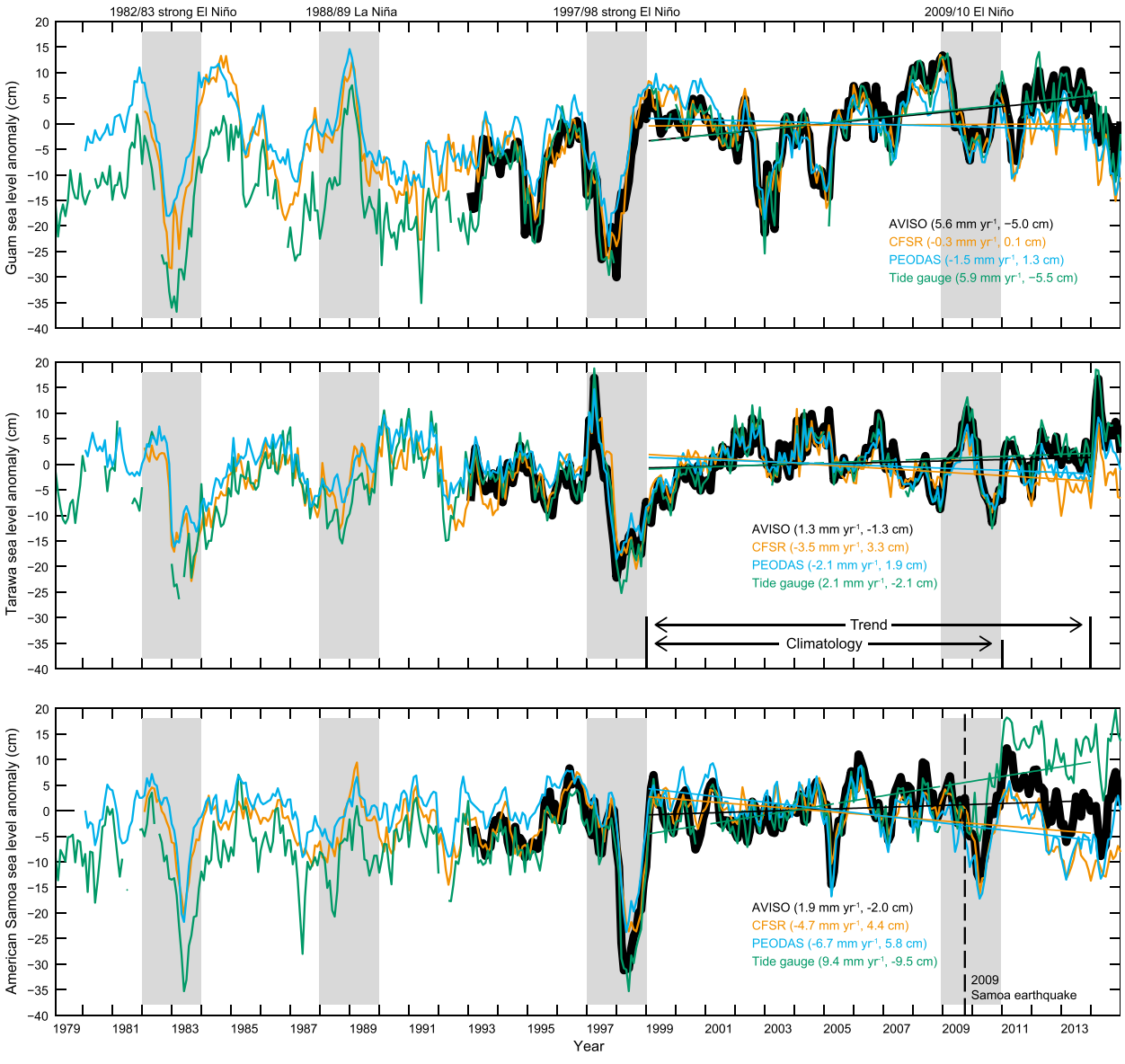

FIG. 2. Observed and simulated sea level anomalies with respect to 1999–2010 climatology from AVISO (1993–2014; black), CFSR (1982–2014; orange), PEODAS (1980–2014; blue), and available tide gauge records (1979–2014; green) around (top) Guam (Apra Harbor), (middle) Tarawa (Betio), and (bottom) American Samoa (Pago Pago). There is close correspondence between sea level products except for differing long-term trends (1999–2013; mm yr^{-1}, see the colored straight lines) for all stations. Trends are especially different around American Samoa since the 2009 earthquake (dashed vertical line in the bottom panel). Trend offsets (cm) added to 2015 real-time forecasts are indicated. El Niño and La Niña events referred to in the text are highlighted.

validated against tide gauge observations as well as satellite-derived measurements and model reanalyses of sea surface height. From January 2015 to the present, we have tested our forecasting system in a real-time framework and provided prediction products via the University of Hawaii Sea Level Center website (http://uhslc.soest.hawaii.edu/products/slforecasts/). The following is a summary of our forecasting methodology, which was successful in predicting many aspects of the sea level response to the development of a strong El Niño event in 2015.

2. Extreme sea level variability

Sea level variability on interannual time scales is well captured throughout the tropical Pacific by tide gauges (e.g., Merrifield et al. 1999), satellite-measured altimetry (e.g., Church and White 2011), and dynamical model

reanalyses of sea surface height (e.g., Miles et al. 2014). We compare in Fig. 1 satellite observations since 1993 (AVISO merged absolute dynamic topography) with simulations used in the assimilation of NOAA's Climate Forecast System, version 2 (CFSv2 for the forecast and CFSR[1] for the reanalysis), and the Predictive Ocean Atmosphere Model for Australia, version 2 [POAMA-2 for the forecast and the POAMA Ensemble Ocean Data Assimilation System (PEODAS)[2] for the reanalysis]. Other than subtle differences in magnitude, the models agree with observations in terms of the patterns of interannual and annual cycle variability in the tropical Pacific. Observations and models reveal the largest interannual variability [Figs. 1a,d,g; standard deviation (SD) $>$ 7 cm] in the tropical western and central Pacific, affecting numerous island nations. Outside the tropical Pacific, interannual variability is underrepresented in the subtropical countercurrent regions of both hemispheres (i.e., offshore of Taiwan and Australia at ~25°N–°S) where ocean eddy processes, which are unresolved in CFSR and PEODAS, produce large sea level anomalies (Xu et al. 2014). Variability of the annual cycle of sea level (Figs. 1b,e,h), which we initially subtract from the observations and our forecasts as it is typically included in tidal predictions already, is smaller and mostly constrained to the equator. The largest annual cycle (SD $\approx$ 10 cm) is organized in horizontal bands adjacent the mean location of wind stress convergence associated with the intertropical convergence zone for AVISO, CFSR, and PEODAS; however, amplitudes exceed 5 cm around many islands even away from the equator (e.g., Guam, located at 14°N). Together, the annual cycle and interannual variability of the Pacific trade winds associated with ENSO (Timmermann et al. 2010) explain most of the monthly mean sea level fluctuations experienced at tropical Pacific islands (Widlansky et al. 2014).

Apparent from historical observations and simulations (Fig. 2) is the close correspondence between satellite measurements and model reanalyses (which do not assimilate data from tide gauges or satellite altimetry) of regional sea level, centered around island tide gauges, for the tropical northwestern Pacific (Guam), equatorial western Pacific (Tarawa), and tropical south-central Pacific (American Samoa). All products recorded below-normal sea levels during the 1982/83 and 1997/98 strong El Niño events. For the later event, interproduct agreement is excellent with the CFSR and PEODAS reanalyses capturing the timing of extreme sea level drops, occurring first around Guam then about six months later around Tarawa and American Samoa, as detected by each tide gauge as well as regional satellite measurements. There are differences among products, however, in magnitude of the sea level anomalies during the earlier years when ocean observations were fewer (e.g., 1984–88 around Guam and American Samoa) and both strong El Niño events (e.g., CFSR and PEODAS underestimate by 10 cm the sea level drop around American Samoa during 1983 and 1998 relative to the island tide gauge). In contrast during 1999–2010, a period of more moderate ENSO events as measured by SST variability in the equatorial eastern Pacific (NOAA ERSST Niño-3.4 peaked at 1.4°C in December 2009 as compared with 2.3°C in November 1997), sea level variability in the reanalyses generally matched the local tide gauges and regional satellite measurements. Agreement between tide gauges, satellite observations, and model reanalyses of the location, magnitude, and temporal evolution of sea level variability gives confidence that dynamical models could be used to develop new prediction tools to complement existing statistical forecasts based solely on tide gauge responses to climate observations (Chowdhury and Chu 2015).

3. Merging observations and model reanalyses

Even though there is strong agreement between observations and reanalyses of the timing and amplitude of sea level variability, the correspondence decays with time away from the center of the climatology period[3] (Fig. 2). Clearly, to achieve a successful multimodel prediction framework, any differences between sea level products must be addressed so that forecasts are free of model-dependent biases.

By model design, there is little agreement on the long-term sea level trend between tide gauge records or satellite measurements (which resolve global sea level rise) and climate model reanalyses (which do not, for example, include the sea level effects of runoff from melting land ice or resolve well the observed

[1] CFSR (Saha et al. 2010) was initialized from the Global Ocean Data Assimilation System (GODAS).

[2] PEODAS (Yin et al. 2011) was initialized from the 40-yr European Centre for Medium-Range Weather Forecasts Re-Analysis (ERA-40).

[3] We choose the period 1999–2010 to place predicted sea level anomalies in a more recent context than if some longer climatology was used (e.g., 1982–2010). The more recent period also allows comparisons with the satellite altimetry record. Additionally, the period 1999–2010 is used by the NCEP Climate Prediction Center for making seasonal forecasts with CFSv2.

ocean thermal expansion) around Guam, Tarawa, American Samoa (Fig. 2), or elsewhere in most of the tropical Pacific (Figs. 1c,f,i). Averaged over changes from 1999 to 2013, satellite measurements reveal that sea levels rose fastest in the tropical northwestern Pacific (Fig. 1c), which is confirmed by tide gauge records (Fig. 2). For Guam, the AVISO trend was 5.6 mm yr^{-1} (5.9 mm yr^{-1}, tide gauge), whereas for Tarawa, the AVISO rise was only 1.3 mm yr^{-1} (2.1 mm yr^{-1} for tide gauge) and was similarly small for American Samoa (1.9 mm yr^{-1} for AVISO). Influenced by land subsidence since an earthquake in 2009, the tide gauge trend in American Samoa is much larger (9.4 mm yr^{-1}). Strangely, during the 1999–2013 period, both CFSR and PEODAS simulated mostly negative sea level trends in the tropical Pacific (Figs. 1f,i), which range regionally and by model (Fig. 2) from -0.3 mm yr^{-1} around Guam (CFSR) to -6.7 mm yr^{-1} around American Samoa (PEODAS). Such discrepancies between observations and the CFSR and PEODAS reanalyses could perhaps be due to model-inherent temporal drifts in the subsurface ocean temperature or other unresolved factors (Miles et al. 2014; Saha et al. 2010).

As there are large sea level trends that vary across products and times, which introduce drifts in predictions from the statistical (sensitive to the tide gauge record) and dynamical (simulation biases) models, we remove the long-term trend from each model's prediction through the following three steps:

1) We calculate the region-specific linear trend for a period sufficient to capture real or artificial sea level changes in each product (e.g., for retrospective as well as 2015 forecasts, trends are calculated from 1999 to 2013).
2) We subtract from retrospective forecasts, for each time, the linear trend respective of model (i.e., trends are either tide gauge derived for statistical forecasts or CFSR–PEODAS derived for dynamical forecasts).
3) We subtract from 2015 predictions the offset between the December 2013 trend value and zero (listed in Fig. 2). Likewise, we subtract from retrospective forecasts prior to January 1999 the offsets between the January 1999 trend value and zero.

Thus, our multimodel predictions are with respect to a uniform climatology period and assume no long-term trends relative to the 1999–2013 period. With this method comes the ability to merge dynamical models with observation-based statistical forecasts, but we note that underestimates of the pre-1999 tide gauge trend do occur (e.g., Guam sea level rise during the 1980s is not completely removed; Fig. 2), which could adversely affect the retrospective forecasts from statistical models for those years. Going forward, the trend period will be extended for subsequent forecast years (e.g., 1999–2014 for predictions made during 2016), but there will always be a separation exceeding one year between the trend and forecast initialization to avoid potential aliasing caused by, for instance, the ENSO sea level signal persisting between years.

4. Retrospective forecast skill

Here we describe each of the forecast models, noting only key aspects of their design and initialization. We then assess the historical performance and uncertainty (1979–2014) of our multimodel sea level anomaly predictions individually and as an ensemble mean, which is based on equal-weighting averages of the five models. To verify our forecasts, we average the tide gauge, satellite altimetry, and two sea level reanalyses to produce one merged analysis of sea level extending back to 1979 (Fig. 3, black line), noting that only since 1993 (AVISO satellite altimetry) are all four products available.[4] Thus, the merged sea level analysis provides a verification that is less sensitive to gaps or errors from any one observation product.

a. *Statistical models*

We employ three statistical models derived independently from (i) canonical correlation analysis (CCA), (ii) multivariate linear regression (MLR), and (iii) artificial neural network (ANN) methods to relate the tropical Pacific climate variability to monthly mean tide gauge anomalies. Each model uses NOAA ERSST, which well captures ENSO variability (Huang et al. 2015), and ''research quality'' tide gauge data from the University of Hawaii Sea Level Center (fast delivery data are used for the real-time forecasts). The CCA model (Chowdhury and Chu 2015) establishes linear relationships between the optimum leading patterns (maximum five) of SST monthly variability, identified using empirical orthogonal function (EOF) analysis of the tropical Pacific (30°N–30°S, 100°E–100°W). The MLR (Rencher and Christensen 2012) and ANN (Billings 2013) models, introduced here for sea level forecasting, are based on a larger sample of SST EOFs (10 leading patterns for 40°N–40°S, 120°E–70°W, which explain over 80% of the total variance). The ANN is the only statistical model to encapsulate the nonlinear relationships between SST and tide gauge records to make the sea level forecasts. Both the

[4] Gaps in the tide gauge records and start dates of CFSR (1982) and PEODAS reanalyses (1980) are shown in Fig. 2.

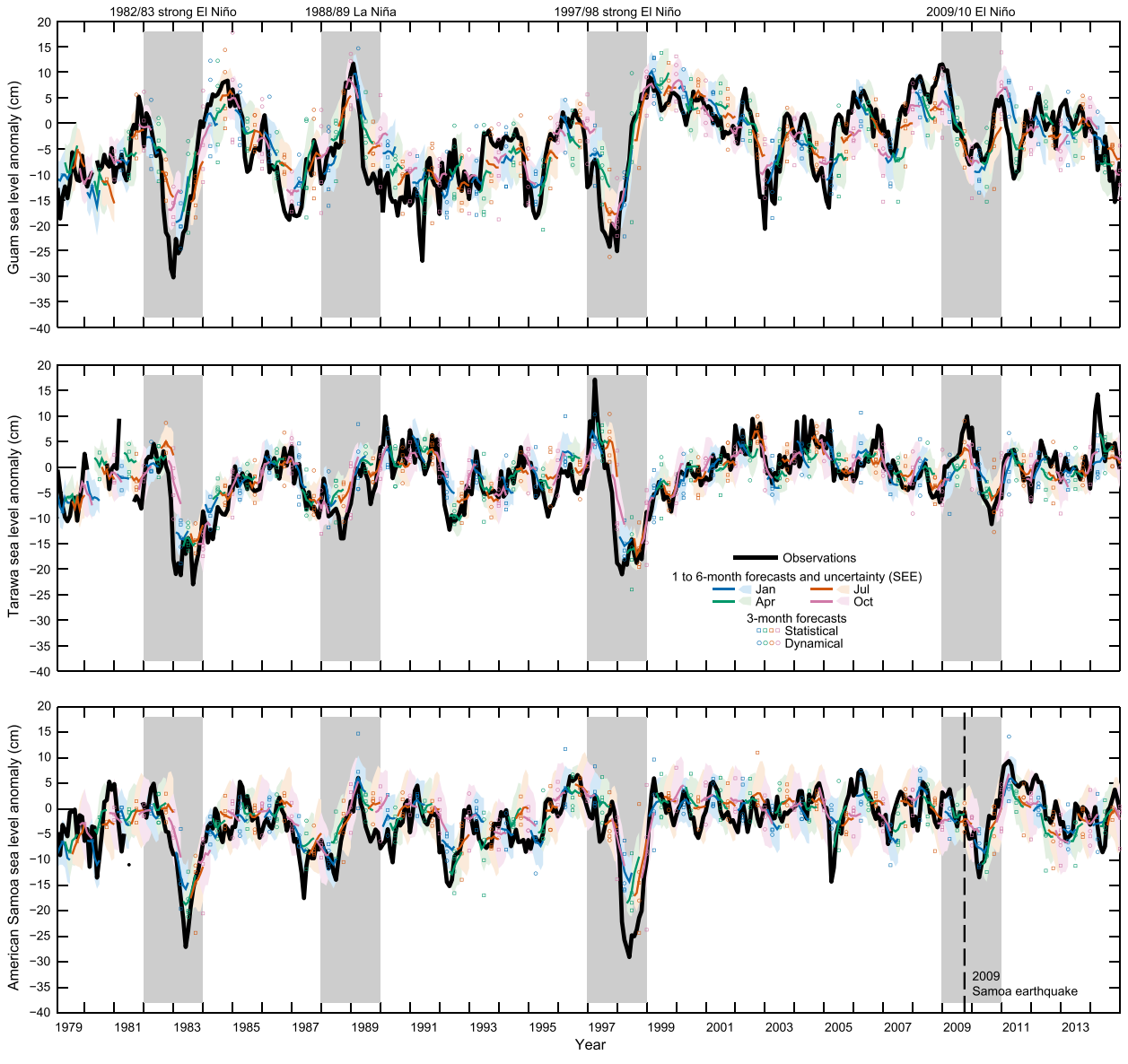

FIG. 3. Retrospective 6-month multimodel sea level forecasts beginning each January (blue), April (green), July (orange), and October (purple) from 1979 to 2014 around (top) Guam, (middle) Tarawa, and (bottom) American Samoa. The observed time series (black) is an average of monthly anomalies from available tide gauges, AVISO satellite altimetry, and two reanalyses of sea surface height (CFSR and PEODAS) with respect to their 1999–2010 climatology. Retrospective ensemble mean forecasts (colored lines) are averages of three statistical models (CCA, MLR, and ANN) and two dynamical models (CFSv2 and POAMA-2). The corresponding ensemble mean SEE (± 1) is shaded. The 3-month lead forecasts for each model are indicated by circles (dynamical) and squares (statistical), colored by start time. Long-term trends (1999–2013) have been removed from observations and forecasts. The 2009 Samoa earthquake is indicated (dashed vertical line in bottom panel). El Niño and La Niña events referred to in the text are highlighted above the top panel.

MLR and ANN models are trained using tide gauge anomalies with the trend removed, whereas the trend is initially retained for CCA then removed a posteriori from that model's retrospective and real-time forecasts.

b. *Dynamical models*

We employ output from two global coupled ocean–atmosphere dynamical models (CFSv2 and POAMA-2) and their respective ocean data assimilation systems (CFSR and PEODAS). Both CFSv2 (Saha et al. 2014) and POAMA-2 (Hudson et al. 2013; McIntosh et al. 2015; Miles et al. 2014) capture sea level contributions due to dynamic height, barotropic circulation, advection, and dissipation processes, using the hydrostatic equations to calculate changes in the sea surface height for each grid on the globe. We extract from these global simulations, as

well as AVISO observations, island-centered regional averages (2° latitude × 2° longitude shown in Fig. 1). POAMA-2, which uses an older version of the ocean model than CFSv2 [the Modular Ocean Model (MOM): MOM2 vs MOM4], does not simulate atmospheric pressure effects, unlike CFSv2, which simulates rising sea surface heights when sea level pressure falls and vice versa (i.e., the inverse barometer effect), potentially explaining some differences between forecasts, especially outside the tropics where large-scale atmospheric pressure variability is larger. We note that the following contributions to monthly sea level anomalies are not simulated by either dynamical model: changes in ocean mass from ice sheet melt, tectonic uplift, self-attraction and loading, glacial isostatic adjustment, land water storage, astronomical tides, surface waves, or mesoscale eddies. Thus, any long-term trends in simulated sea level (Figs. 1f,i), which we remove, must be considered potentially as errors introduced by artificial model drifts.

To achieve equal weighting for each model, multiple forecast runs generated by the dynamical model centers are averaged every month. CFSv2 retrospective forecasts consist of four initializations every fifth day (292 runs per year), whereas real-time forecasts are initialized four times daily. From both retrospective and real-time forecasts, we subtract a smoothed climatology calculated from the pentad retrospective forecasts, as in Saha et al. (2014), then average the past 30 days each month. For POAMA-2, which is run every four days in retrospective and real time, we use an ensemble of 33 members created from slightly different initial conditions on the last forecast day in a particular month. Thus, our multimodel forecast contains a trade-off between CFSv2's larger ensemble size (120 start times spread evenly across an entire month) versus POAMA-2's smaller ensemble started later in the month, which would conceivably often yield higher forecast skills, at least for leads close to the start time (i.e., a 1-month outlook).

c. *Multimodel predictions and uncertainty*

We assembled retrospective forecasts (Fig. 3; 1979–2014), or hindcasts, initialized four times per year (December$_{\text{year}-1}$, March, June, and September) for each model and assessed their predictive skill individually, by category (statistical or dynamical ensemble averages), and as a multimodel ensemble mean (Table 1 and Fig. 4) out to six months (January–June, April–September, July–December, and October–March$_{\text{year}+1}$). Since 1979, the ensemble mean predicts the extreme sea level drops during strong El Niño (1982/83 and 1997/98) events as well as many of the smaller negative and positive anomalies associated with weaker El Niño (e.g., 2009/10) and La Niña (e.g., 1988/89) events, respectively. The timing of the largest sea level changes is also well captured (i.e., extreme sea level drops are predicted first in the northwestern Pacific around Guam during boreal fall, followed about six months later toward the south around Tarawa and American Samoa), demonstrating predictability of the meridional sea level seesaw that is observed with strong El Niño (Widlansky et al. 2014). Perhaps most important from a reliability perspective, there are no false extremes (very high or low sea level stands not matched in the observations) in the ensemble mean predictions.

Multimodel averaging typically cancels individual model errors (Jin et al. 2008), which are often caused by amplitudes that are too large relative to observations, even at only 3-month leads (Fig. 3). Whereas forecast skill generally improves with increasing model sophistication, as indicated by higher anomaly correlation coefficients (ACCs) and lower root-mean-square errors (RMSEs) moving from top to bottom in Table 1, skill of the different ensemble averages (statistical, dynamical, or both model types) is usually higher than the best-performing model in the respective ensemble subset. The advantage of a multimodel ensemble (even with a small sample size) is apparent by comparing the skill of CFSv2 and POAMA-2 individually—two dynamical models that perform similarly well—with that from when their predictions are averaged together (Table 1). More often than not, skill of the dynamical ensemble mean beats the best-performing dynamical model for a particular region and forecast month (16/24 ACC and RMSE scores at 3-month lead and 14/24 at 6-month lead). Including the statistical models yields mixed results, mostly improving predictions for Guam and Tarawa (higher ACC, lower RMSE at 3- and 6-month leads) but worsening the predictive skill for American Samoa. Clearly, however, the multimodel ensemble mean provides a robust prediction of sea level anomalies out to six months (ACC > 0.7 for 9/12 scores and RMSE $<$ 6 cm for 11/12 scores) that beats simple climatology or persistence forecasts for the tropical Pacific island regions that we analyzed (Table 1 and Fig. 4).

Interestingly, performance of the multimodel ensemble mean forecast varies by location as well as season (Fig. 4). For Guam, the ACC of 6-month forecasts is higher for July ($r = 0.83$) and October ($r = 0.84$) start times than for January ($r = 0.59$) and April ($r = 0.72$), which perform worse, likely because of the so-called spring predictability barrier in forecasting the development of El Niño (e.g., Webster 1995) and associated sea level drops in the tropical northwestern Pacific (e.g.,

TABLE 1. Retrospective forecast skills measured by ACC and RMSE (in parentheses) at 3- and 6-month leads for the three island regions and four start times. Models are organized by increasing complexity (climatology and persistence forecasts are not included in the ensemble mean). Bold values indicate skills higher than from the respective persistence forecast.

		Skill at 3-month lead: ACC (RMSE)			Skill at 6-month lead: ACC (RMSE)		
Model	Hindcast start	Guam	Tarawa	American Samoa	Guam	Tarawa	American Samoa
Climatology (statistical)	Jan	— (9.6)	— (7.6)	— (8.2)	— (8.1)	— (5.5)	— (7.8)
	Apr	— (8.1)	— (5.5)	— (7.8)	— (8.8)	— (7.0)	— (5.7)
	Jul	— (8.8)	— (7.0)	— (5.7)	— (11.3)	— (6.4)	— (4.6)
	Oct	— (11.3)	— (6.4)	— (4.6)	— (9.5)	— (7.6)	— (8.3)
Persistence (statistical)	Dec	0.87 (5.0)	0.62 (6.3)	0.46 (7.0)	0.46 (9.2)	0.48 (5.7)	0.33 (6.9)
	Mar	0.61 (6.8)	0.79 (4.9)	0.77 (5.3)	0.30 (9.5)	0.73 (5.4)	0.59 (6.4)
	Jun	0.63 (6.2)	0.85 (3.6)	0.77 (4.5)	0.47 (9.0)	0.30 (6.5)	0.25 (7.1)
	Sep	0.88 (5.0)	0.49 (6.3)	0.56 (4.4)	0.75 (5.7)	0.12 (9.5)	−0.06 (9.7)
CCA (statistical)	Jan	0.66 (6.4)	**0.73 (5.2)**	**0.73 (5.7)**	0.24 (**7.4**)	**0.73 (3.3)**	**0.56 (6.1)**
	Apr	0.40 (7.0)	0.78 (**3.1**)	0.49 (7.0)	0.16 (**8.4**)	0.60 (**5.3**)	0.27 (6.5)
	Jul	0.51 (6.9)	0.66 (5.0)	0.28 (6.4)	**0.56 (8.6)**	0.06 (**6.3**)	−0.13 (**6.5**)
	Oct	0.62 (8.4)	0.27 (**6.0**)	−0.04 (6.2)	0.60 (6.9)	**0.72 (5.4)**	**0.64 (6.6)**
OLS (statistical)	Jan	0.79 (5.4)	**0.83 (4.5)**	**0.79 (5.1)**	**0.54 (6.5)**	**0.84 (2.9)**	**0.71 (4.9)**
	Apr	**0.65 (6.1)**	0.77 (**3.8**)	0.73 (**4.7**)	**0.66 (6.5)**	0.71 (**4.7**)	**0.72 (3.7)**
	Jul	**0.79 (4.8)**	0.72 (4.6)	**0.81 (3.2)**	**0.78 (6.4)**	**0.34 (6.1)**	**0.26 (4.7)**
	Oct	0.69 (7.4)	**0.62 (4.9)**	0.51 (**4.1**)	0.68 (6.2)	**0.73 (5.2)**	**0.71 (5.9)**
ANN (statistical)	Jan	0.84 (5.3)	0.58 (**6.2**)	**0.58** (7.5)	0.42 (**6.6**)	**0.51 (4.6)**	**0.40** (7.7)
	Apr	0.56 (**5.8**)	**0.84 (2.9)**	0.75 (5.9)	**0.37 (7.5)**	**0.79 (4.2)**	**0.66 (5.0)**
	Jul	**0.69 (5.9)**	**0.86** (4.0)	**0.81 (3.6)**	**0.52 (8.9)**	**0.32 (6.2)**	**0.33 (4.2)**
	Oct	0.81 (7.6)	**0.53 (5.3)**	0.48 (**3.8**)	0.65 (6.7)	**0.15 (8.1)**	**0.20 (8.3)**
Ensemble mean (statistical)	Jan	0.80 (**5.0**)	**0.84 (4.5)**	**0.79 (5.3)**	**0.48 (6.0)**	**0.84 (2.7)**	**0.64 (5.4)**
	Apr	0.60 (**5.5**)	**0.88 (2.4)**	0.67 (**5.2**)	**0.52 (6.6)**	**0.78 (4.3)**	0.58 (**4.5**)
	Jul	**0.73 (5.3)**	0.81 (4.2)	0.71 (**3.8**)	**0.71 (7.2)**	0.27 (**6.0**)	0.11 (**4.7**)
	Oct	0.76 (6.7)	**0.58 (4.9)**	0.35 (**4.1**)	0.75 (5.7)	**0.75 (5.2)**	**0.70 (6.1)**
POAMA-2 (dynamical)	Jan	0.81 (6.5)	**0.77 (4.8)**	**0.88 (4.3)**	**0.48 (6.9)**	**0.77 (3.4)**	**0.83 (4.4)**
	Apr	**0.70 (5.6)**	**0.90 (2.7)**	**0.81 (4.5)**	**0.73 (5.9)**	**0.84 (4.2)**	**0.72 (3.7)**
	Jul	**0.86 (5.0)**	0.83 (4.0)	0.74 (**3.7**)	**0.78 (8.3)**	**0.54 (5.3)**	**0.49 (3.7)**
	Oct	0.84 (7.4)	**0.72 (4.6)**	**0.56 (3.7)**	**0.79** (6.7)	**0.80 (4.9)**	**0.77 (5.4)**
CFSv2 (dynamical)	Jan	**0.90 (4.0)**	**0.80 (4.7)**	**0.77 (5.2)**	**0.48 (6.6)**	**0.69 (3.8)**	**0.75 (4.9)**
	Apr	**0.69 (5.4)**	0.72 (**3.5**)	**0.81 (4.1)**	**0.62 (7.5)**	**0.83 (3.7)**	0.51 (**4.7**)
	Jul	**0.91 (3.9)**	0.83 (3.9)	**0.78 (3.3)**	**0.84 (6.4)**	**0.50 (5.5)**	**0.40 (4.3)**
	Oct	0.85 (6.1)	**0.61 (4.9)**	**0.62 (3.2)**	**0.89 (4.8)**	**0.70 (5.6)**	**0.75 (5.5)**
Ensemble mean (dynamical)	Jan	**0.91 (4.5)**	**0.85 (4.1)**	**0.86 (4.4)**	**0.61 (6.4)**	**0.75 (3.5)**	**0.83 (4.3)**
	Apr	**0.75 (5.1)**	**0.87 (2.6)**	**0.86 (3.9)**	**0.71 (6.3)**	**0.85 (3.6)**	**0.72 (3.8)**
	Jul	**0.90 (4.3)**	**0.87 (3.4)**	**0.83 (3.1)**	**0.83 (7.0)**	**0.56 (5.1)**	**0.57 (3.5)**
	Oct	0.85 (6.5)	**0.76 (4.0)**	**0.67 (3.0)**	**0.87 (5.6)**	**0.80 (4.9)**	**0.83 (5.0)**
Multimodel ensemble mean	Jan	**0.88 (4.2)**	**0.88 (4.1)**	**0.84 (4.7)**	**0.59 (5.4)**	**0.86 (2.7)**	**0.72 (4.9)**
	Apr	**0.76 (4.4)**	**0.90 (2.2)**	0.76 (**4.6**)	**0.72 (5.6)**	**0.84 (3.8)**	**0.70 (4.0)**
	Jul	**0.87 (4.2)**	**0.89 (3.4)**	**0.78 (3.4)**	**0.83 (6.4)**	**0.40 (5.5)**	**0.30 (4.1)**
	Oct	0.86 (5.8)	**0.69 (4.4)**	0.51 (**3.6**)	**0.84 (5.0)**	**0.85 (4.8)**	**0.78 (5.5)**

Wyrtki 1984). The 6-month persistence of boreal fall sea level anomalies around Guam is also much longer than spring persistence ($r = 0.75$ vs $r = 0.30$; September and March persistence, respectively) whereas around Tarawa and American Samoa, the seasonal dependence is reversed ($r = 0.12$ and $r = -0.06$ for March and September persistence, respectively). Likewise, the spring predictability barrier is not evident in the Tarawa and American Samoa sea level forecasts, although July starts suffer much poorer skills at a 6-month lead ($r = 0.40$ and $r = 0.30$) when compared with those of other start times. Such a complicated performance of the retrospective forecasts necessitates defining skill metrics, which are start-time dependent, to fully describe seasonally varying uncertainty.

Rather than using the ensemble spread between predictions from individual models to quantify forecast uncertainty, which would be limited by our small ensemble size (five models), we instead follow the methodology in Barnston et al. (2015) to measure the hindcast correlation skill (cor_{xy}, here computed using the multimodel mean prediction) and relate that to the

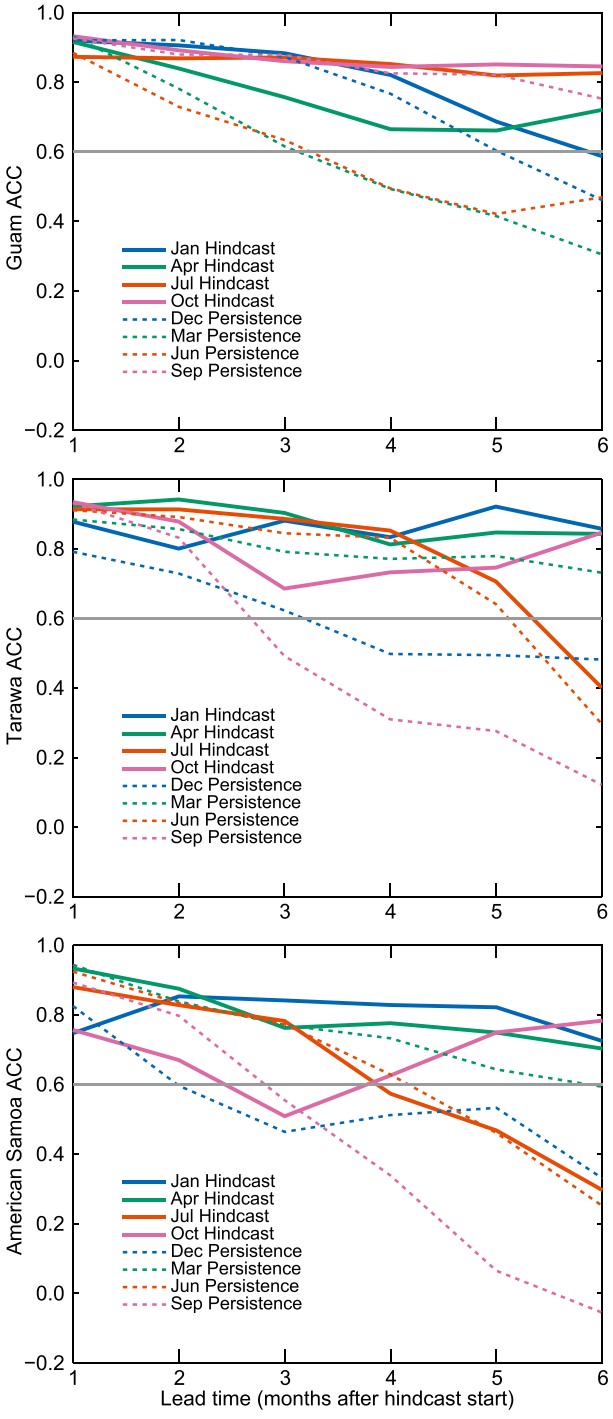

FIG. 4. Retrospective forecast skill of the multimodel ensemble mean measured by ACC for predictions beginning each January (blue), April (green), July (orange), and October (purple) from 1979 to 2014 around (top) Guam, (middle) Tarawa, and (bottom) American Samoa. Corresponding persistence forecasts are indicated by dashed lines. For reference, the gray horizontal line indicates $r = 0.6$ (36% variance explained).

standard deviation of the observations (SD_y) for different lead times. This uncertainty metric, called the standard error of estimate [$SEE = SD_y(1 - cor_{xy}^2)^{1/2}$], varies by forecast start time and target month but does not change from year to year, reflecting a constant underlying signal-to-noise ratio. In general, the SEE captures the observed variability (Fig. 3), but there are a few times when sea level anomalies fall well outside the predicted uncertainty estimate. The extreme sea level drop around American Samoa in 1998 (during termination of a strong El Niño event; Widlansky et al. 2014) and the abrupt rise around Tarawa during early 2014 (a series of westerly wind bursts triggered a downwelling equatorial Kelvin wave at this time, which briefly lowered the thermocline depth, thus elevating sea surface near the equator; Menkes et al. 2014) are two notable examples when our multimodel hindcasts underpredicted the anomalies, even for start times near the event peaks.

5. Real-time forecasts

To illustrate the state of our multimodel sea level predictions, we discuss an example forecast issued during July 2015 covering the remainder of that year as El Niño developed into a strong event (NOAA ERSST Niño-3.4 peaked at 2.4°C, the highest ever recorded, in November 2015). Figures 5a–c show, for Guam, Tarawa, and American Samoa, the ensemble mean and individual model predictions produced from multimodel initializations one month prior to issuing the forecast (June). From the skill of the 1979–2014 retrospective forecasts starting in July (Table 1 and Fig. 4), and specifically their performance during the development of past strong El Niño events, we would expect a well-performing ensemble mean forecast at three months' lead for all regions (ACC between 0.78 and 0.89; RMSE between 3.4 and 4.2 cm) and skill extending to six months for Guam (ACC = 0.83). Much lower performance is expected for Tarawa and American Samoa (ACC = 0.40 and 0.30, respectively) that is made worse by the statistical models, which struggle most at this forecast time for 6-month leads (Table 1). Such forecast uncertainty is included with the real-time predictions using the SEE metric, which is especially large for American Samoa at longer leads (low cor_{xy} and high SD_y) but smaller for Guam and Tarawa (orange shading, Fig. 5).

Guam, like the neighboring islands in the tropical northwestern Pacific (Figs. 5d–f), experienced below-normal sea levels for all of 2015. Wide expanses of shallow coastal reefs were exposed during a series of low tides, especially in October, when the lowest sea level occurred. In July, we predicted that Guam sea levels would fall further (Fig. 5a); however, only the CFSv2

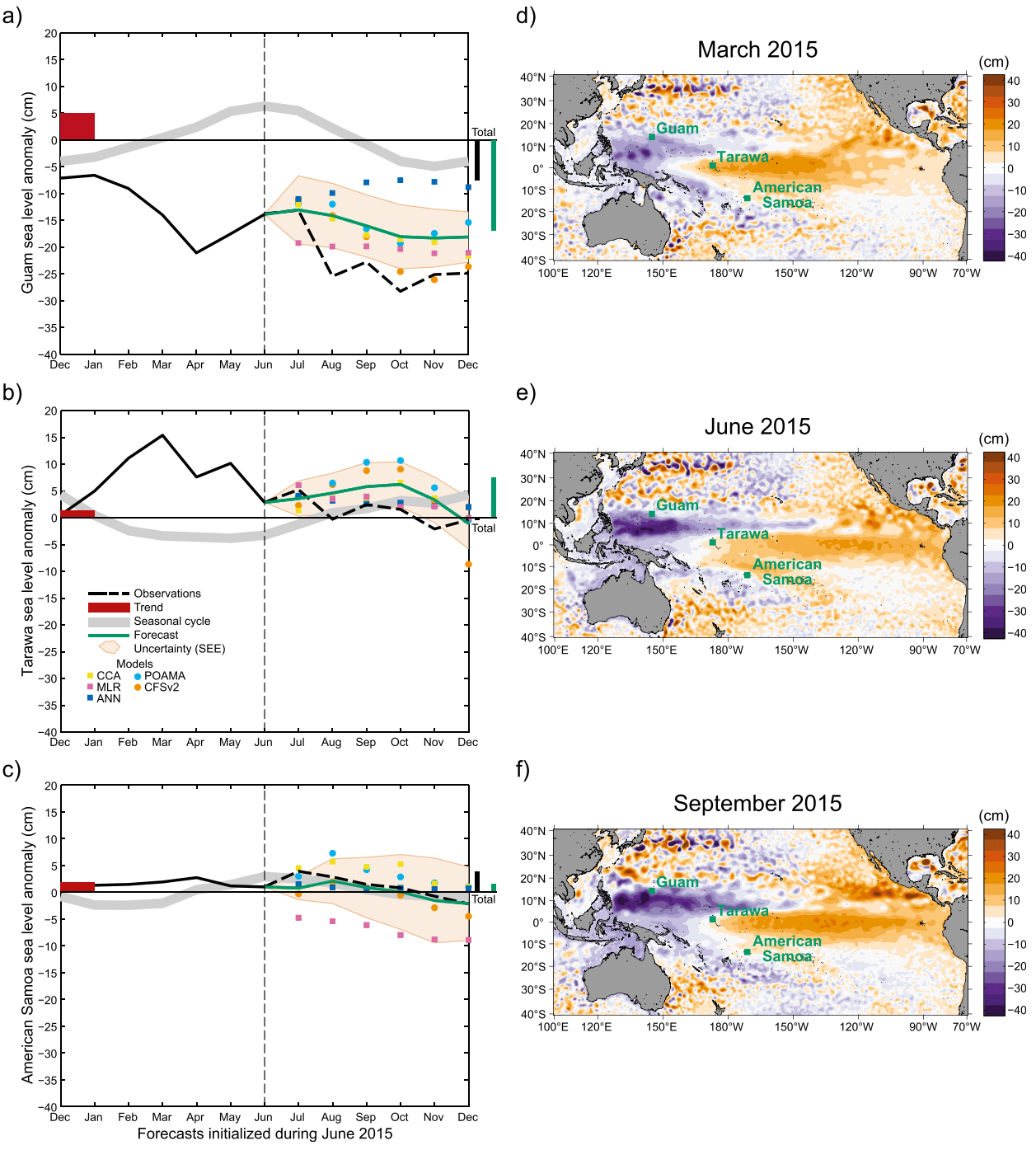

FIG. 5. Multimodel sea level forecasts for July–December 2015 around (a) Guam, (b) Tarawa, and (c) American Samoa. The ensemble mean forecast (green) is an average of three statistical models (CCA, MLR, and ANN; squares colored yellow, magenta, and dark blue, respectively) and two dynamical models (CFSv2 and POAMA-2; circles; orange and light blue, respectively). Shading indicates the corresponding ensemble mean SEE (±1). The long-term trend value (red) and seasonal cycle (gray) for each region (calculated from AVISO satellite altimetry) are indicated. Vertical bars outside the panels indicate the total sea level anomaly (trend + seasonal cycle + monthly anomaly) observed for the initialization month (June; black) and predicted using the 2–4-month forecast average (August–October; green). The observed time series is shown in solid and dashed black for the pre- and postforecast verification, respectively, and is an average of monthly anomalies from: available tide gauges, AVISO satellite altimetry, and two analyses of sea surface height (CFSR and PEODAS) with respect to their 1999–2010 climatology. Also shown are observed sea surface height anomalies (AVISO) during (d) March, (e) June, and (f) September 2015.

dynamical model captured the extreme drop that exceeded −25 cm and was below the SEE lower bound.

Sea levels in the equatorial central Pacific around Tarawa peaked near +15 cm during March 2015 (Figs. 5b,d), which was similar to the rise recorded there during early 2014 (Fig. 2), before lowering to near normal by the end of the year (Figs. 5b,f), mirroring the ocean thermocline changes as Kelvin waves transported warm water eastward, fueling El Niño. Interestingly, the statistical models captured the gradual falling sea level, whereas both the POAMA-2 and CFSv2 dynamical models kept sea levels too high from August to October[5] before dropping abruptly in November and December (5–6-month lead) as El Niño peaked.

Sea level anomalies in the South Pacific, especially around American Samoa (Fig. 5c), stayed near zero for all of 2015 in satellite observations (Figs. 5d–f). As all of our statistical models are trained with historical data and then, for CCA and ANN, predictions are initialized each month from real-time tide gauge observations, retrospective forecasts for American Samoa (Fig. 3) after 2009 were biased by the postearthquake land subsidence, with prediction errors becoming worse with further sinking over time (MLR uses observations only for training as this model is not initialized from the most recent observation). Using an estimate of the vertical land motion (−11.8 cm; 2012–15 average difference between regional satellite altimetry and the Pago Pago tide gauge), we adjusted the tide gauge datum, successfully removing most of the postearthquake drift. Rerunning our statistical models for 2015 with this ''unofficial'' tide gauge correction yields better agreement with the dynamical models (Fig. 5c), which are unaffected by the datum change, and verifies on average with observations for our July 2015 real-time forecast. After the peak of past strong El Niño events, the large meridional sea level gradient between Guam and American Samoa reversed dramatically as sea levels dropped in the south-central Pacific but returned to normal in the northwest Pacific (Widlansky et al. 2014). Our forecasts initialized later in 2015 provided an early warning of such a change during 2016.

From our real-time forecasts (Figs. 5a–c) comes the best estimate for the next six months of the total sea level anomaly, which is the sum of (i) the observed long-term trend, (ii) the seasonal cycle, and (iii) the multimodel predicted monthly anomalies. Since extreme total water levels mostly occur on time scales shorter than a month and are often exacerbated by tidal fluctuations, there is a need to combine the climate-driven sea level anomalies that we forecast with existing astronomical tide predictions. Stephens et al. (2014) illustrated the potential use of such an early warning sea level calendar, showing that inclusion of sea level anomaly forecasts enhances the prediction of tide levels with a more realistic connection to what actually may occur. Figure 6 shows the predicted tides for Guam during October 2015 with or without the total sea level anomaly that we predicted three months prior (i.e., the July 2015 forecast; Fig. 5a). Even though there has been substantial long-term sea level rise around Guam (5 cm, 1999–2013; red bar in Fig. 5a), the predicted below-normal sea level (−18 cm; green line in Fig. 5a) associated with strong El Niño, combined with low seasonal sea levels that are typically observed during October (−4 cm; gray line in Fig. 5a) and which are already factored into the harmonic tidal prediction (Codiga 2011), would not only lower the monthly mean sea level but also increase the number of expected extreme low tides relative to the astronomical prediction alone (one vs six events lower than the lowest 5% of historical astronomical tides). Adding to the tide prediction, our multimodel total sea level anomaly forecast (long-term trend plus monthly anomaly), in this example, would have decreased the residual between observed and predicted hourly sea levels around Guam (−15 vs −2 cm monthly average; Fig. 6b), thus providing a more accurate outlook of the potential for coastal reef exposures, which were widely reported during October 2015.

6. Conclusions and future applications

Clear differences in performance of the statistical and dynamical models are apparent from the retrospective forecasts (Fig. 3 and Table 1), although the example real-time forecasts issued during 2015 (Figs. 5a–c) illustrate that intermodel differences are not always systematic. As sea level predictions from additional coupled ocean–atmosphere models become available (e.g., from the North American Multimodel Ensemble type experiments; Kirtman et al. 2014), it would be informative to distinguish the statistical versus dynamical ensemble average as each model type has different forecast skill, which varies by location and lead. Thus, increasing the ensemble size and applying more sophisticated intermodel weighting techniques are likely ways forward to improved forecasts, in addition to incremental improvements of the dynamical models themselves [e.g., POAMA-2's successor, ACCESS-Seasonal (ACCESS-S), is scheduled to be operational in 2017] that will provide higher

[5] The NCEP Climate Prediction Center identified a bug in the CFSv2 initialization process that developed during 2015—since fixed—which was found to be causing El Niño to persist too long; however, it has not been determined how exactly this affected Pacific sea level forecasts.

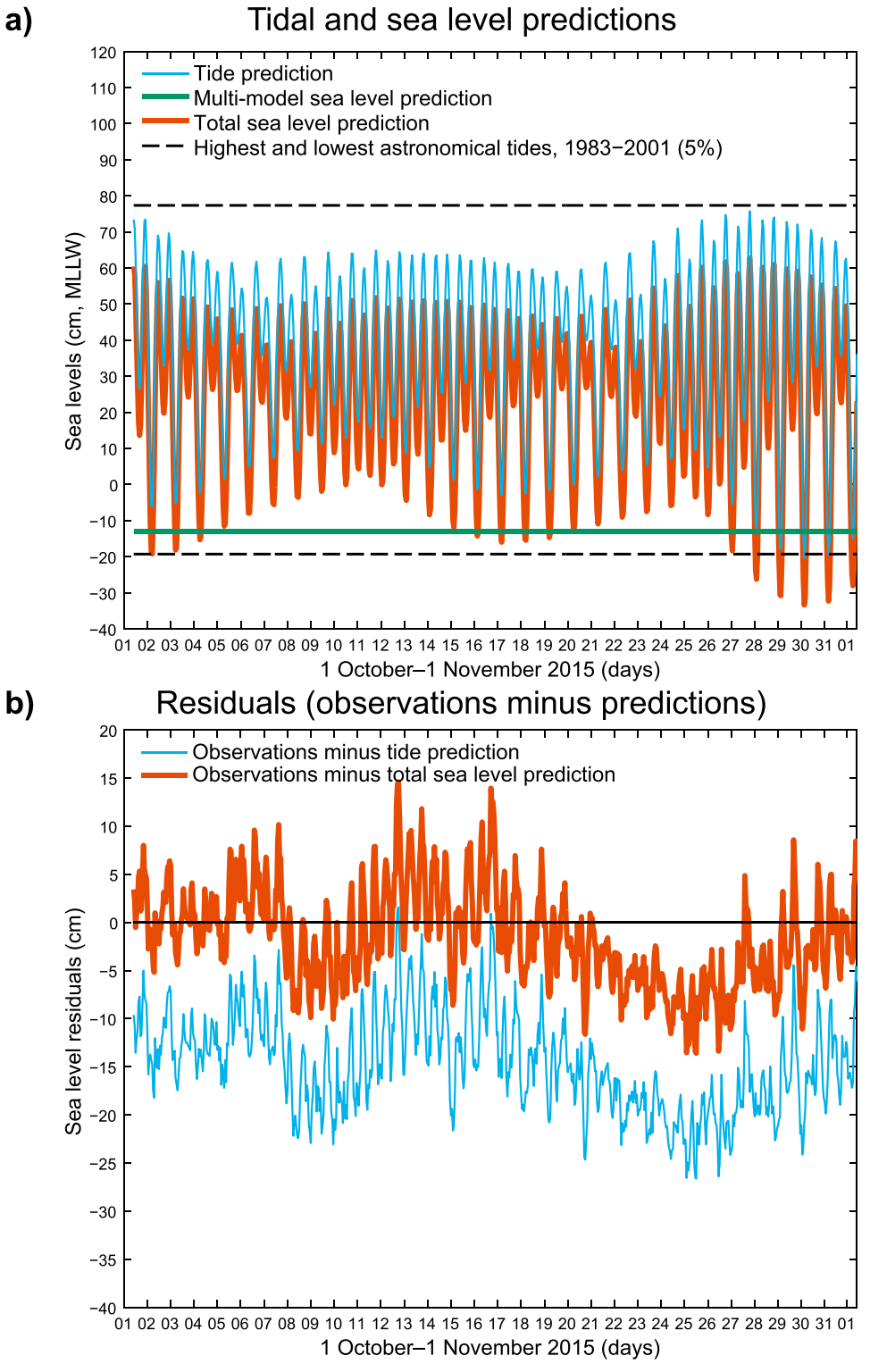

FIG. 6. Hourly sea levels (cm) for Guam during October 2015. (a) Tide predictions (blue) are based on harmonic analysis of the Apra Harbor sea level recorded during the National Tidal Datum Epoch (NTDE; 1983–2001) with the long-term trend removed. The total sea level prediction (orange) combines the expected tides with our multimodel mean sea level anomaly prediction (green) and the long-term trend (5 cm; Fig. 5a). For reference, the highest and lowest 5% of astronomical tides during NTDE are shown (dashed horizontal lines). Sea levels are with respect to the mean lower low water (MLLW) datum. (b) Residuals between the observed sea levels and either the tide prediction (blue) or the total sea level prediction (orange).

horizontal resolutions, which may be especially important for predicting sea levels in the subtropical western Pacific where ocean eddy processes are important as well as along continental coastlines where nearshore processes have so far been mostly unresolved.

To improve stakeholder applicability of our sea level forecasts, we are in the process of (i) expanding the forecast domain and (ii) applying the sea level anomaly predictions to assess coastal risks. We describe below these applications along with remaining technical hurdles associated with each:

1) *Expanding sea level forecasts to additional coastal communities.* The spatial coverage of our forecasts is primarily limited by the availability of monthly tide gauge observations, which are prescribed to the statistical models and used to cross validate the dynamical models, although satellite altimetry could become a surrogate for regions without a nearby tide gauge. Including Guam, Tarawa, and American Samoa described here, we are serving online monthly forecasts for 12 Pacific islands with plans to explore adding coastal cities on the Pacific coasts of Australia, North America, and South America. Before forecasting for a new region, we must verify each model's ability to simulate processes governing local sea level variability [e.g., river discharges (Moftakhari et al. 2016) or nearshore Kelvin waves (Ryan et al. 2005) sometimes dominate sea level fluctuations along parts of the California coast].
2) *Incorporating predicted monthly mean sea level anomalies into coastal inundation and exposure risk models.* Tide and sea level anomaly predictions (e.g., Fig. 6 and Stephens et al. 2014) can provide a practical early warning tool to assist with management of potential coastal inundation or exposure events. Beyond using our forecasts to provide a basis for such general high or low sea level alerts, relating our sea level forecasts to specific coastal risks will require referencing the total sea level anomalies to local vertical data. For example, we predicted that below-normal sea levels around Guam would increase the number of extreme low tides during October 2015 (Fig. 6), but without a measure of the height of coastal reefs, there was no way to quantify how much coral was at risk of exposure. Height measurement of the built environment (e.g., roads, building foundations, and piers), as it relates to sea level anomalies, would likewise provide a way forward to relate forecasts of high sea level stands to the extent of coastal flood damage expected along a particular shoreline.

Extreme ENSO-related sea level variability, which is projected to become more frequent in the tropical Pacific with greenhouse warming by the majority of current-generation climate models (Widlansky et al. 2015), will accelerate the regional risks posed by waves or storm surges, global sea level rise, and any future land subsidence. Better predictability of sea level fluctuations examined in this study will aid Pacific coastal communities in adapting to not only the impacts of rising sea levels caused by climate change but also shorter-term climate events such as 2015/16 El Niño.

Acknowledgments. We acknowledge Shikiko Nakahara at the University of Hawaii Sea Level Center for processing most of the tide gauge data. Special thanks are given to Paul Davill for providing fast delivery of sea level data for tide gauge stations managed by the Australian Bureau of Meteorology. The altimeter products were produced by Ssalto/Duacs and distributed by Aviso, with support from Cnes (http://www.aviso.altimetry.fr/duacs/). NOAA's CFSR and CFSv2 data were downloaded from the IRI/LDEO Climate Data Library. In addition to regional partners of the "Integrated Water Level Service" who provided valuable discussions, we thank the climate modeling groups at the Australian Bureau of Meteorology (PEODAS and POAMA-2), U.S. Pacific ENSO Applications Climate Center (CCA), and New Zealand National Institute of Water and Atmospheric Research (MLR and ANN) for producing and making available their model output.

MJW was supported by the NOAA Climate Program Office through the University of Hawaii Sea Level Center (NA11NMF4320128) and by the U.S. Department of the Interior through the Pacific Islands Climate Science Center (G15AP00140). SAS and NF were supported by National Institute of Water and Atmospheric Research core funded projects CLCP1305 and CLCP1407.

REFERENCES

Barnston, A. G., M. K. Tippett, H. M. Van den Dool, and D. A. Unger, 2015: Toward an improved multimodel ENSO prediction. *J. Appl. Meteor. Climatol.*, **54**, 1579–1595, doi:10.1175/JAMC-D-14-0188.1.

Becker, J. M., M. A. Merrifield, and M. Ford, 2014: Water level effects on breaking wave setup for Pacific island fringing reefs. *J. Geophys. Res. Oceans*, **119**, 914–932, doi:10.1002/2013JC009373.

Becker, M., B. Meyssignac, C. Letetrel, W. Llovel, A. Cazenave, and T. Delcroix, 2012: Sea level variations at tropical Pacific islands since 1950. *Global Planet. Change*, **80–81**, 85–98, doi:10.1016/j.gloplacha.2011.09.004.

Billings, S. A., 2013: *Nonlinear System Identification: NARMAX Methods in the Time, Frequency, and Spatio-Temporal Domains*. Wiley, 574 pp.

Chowdhury, M. R., and P.-S. Chu, 2015: Sea level forecasts and early-warning application: Expanding cooperation in the South

Pacific. *Bull. Amer. Meteor. Soc.*, **96**, 381–386, doi:10.1175/BAMS-D-14-00038.1.

——, ——, and T. Schroeder, 2007: ENSO and seasonal sea-level variability—A diagnostic discussion for the U.S.-affiliated Pacific Islands. *Theor. Appl. Climatol.*, **88**, 213–224, doi:10.1007/s00704-006-0245-5.

——, ——, and C. C. Guard, 2014: An improved sea level forecasting scheme for hazards management in the US-affiliated Pacific Islands. *Int. J. Climatol.*, **34**, 2320–2329, doi:10.1002/joc.3841.

Church, J. A., and N. J. White, 2011: Sea-level rise from the late 19th to the early 21st century. *Surv. Geophys.*, **32**, 585–602, doi:10.1007/s10712-011-9119-1.

——, and Coauthors, 2013: Sea level change. *Climate Change 2013: The Physical Science Basis*, T. F. Stocker et al., Eds., Cambridge University Press, 1137–1216.

Codiga, D. L., 2011: Unified tidal analysis and prediction using the UTide MATLAB functions. University of Rhode Island Graduate School of Oceanography Tech. Rep. 2011-01, 59 pp.

Huang, B., and Coauthors, 2015: Extended reconstructed sea surface temperature version 4 (ERSST.v4). Part I: Upgrades and intercomparisons. *J. Climate*, **28**, 911–930, doi:10.1175/JCLI-D-14-00006.1.

Hudson, D., A. G. Marshall, Y. Yin, O. Alves, and H. H. Hendon, 2013: Improving intraseasonal prediction with a new ensemble generation strategy. *Mon. Wea. Rev.*, **141**, 4429–4449, doi:10.1175/MWR-D-13-00059.1.

Jin, E. K., and Coauthors, 2008: Current status of ENSO prediction skill in coupled ocean–atmosphere models. *Climate Dyn.*, **31**, 647–664, doi:10.1007/s00382-008-0397-3.

Keener, V. W., J. J. Marra, M. L. Finucane, D. Spooner, and M. H. Smith, Eds., 2012: Climate change and Pacific islands: Indicators and impacts. Pacific Islands Regional Climate Assessment Rep., 170 pp.

Kirtman, B. P., and Coauthors, 2014: The North American Multimodel Ensemble: Phase-1 seasonal-to-interannual prediction; Phase-2 toward developing intraseasonal prediction. *Bull. Amer. Meteor. Soc.*, **95**, 585–601, doi:10.1175/BAMS-D-12-00050.1.

Landerer, F. W., P. J. Gleckler, and T. Lee, 2014: Evaluation of CMIP5 dynamic sea surface height multi-model simulations against satellite observations. *Climate Dyn.*, **43**, 1271–1283, doi:10.1007/s00382-013-1939-x.

McIntosh, P. C., J. A. Church, E. R. Miles, K. Ridgway, and C. M. Spillman, 2015: Seasonal coastal sea level prediction using a dynamical model. *Geophys. Res. Lett.*, **42**, 6747–6753, doi:10.1002/2015GL065091.

McPhaden, M. J., A. Timmermann, M. J. Widlansky, M. A. Balmaseda, and T. N. Stockdale, 2015: The curious case of the El Niño that never happened: A perspective from 40 years of progress in climate research and forecasting. *Bull. Amer. Meteor. Soc.*, **96**, 1647–1665, doi:10.1175/BAMS-D-14-00089.1.

Menkes, C. E., M. Lengaigne, J. Vialard, M. Puy, P. Marchesiello, S. Cravatte, and G. Cambon, 2014: About the role of westerly wind events in the possible development of an El Niño in 2014. *Geophys. Res. Lett.*, **41**, 6476–6483, doi:10.1002/2014GL061186.

Merrifield, M., B. Kilonsky, and S. Nakahara, 1999: Interannual sea level changes in the tropical Pacific associated with ENSO. *Geophys. Res. Lett.*, **26**, 3317–3320, doi:10.1029/1999GL010485.

——, P. R. Thompson, and M. Lander, 2012: Multidecadal sea level anomalies and trends in the western tropical Pacific. *Geophys. Res. Lett.*, **39**, L13602, doi:10.1029/2012GL052032.

Miles, E. R., C. M. Spillman, J. A. Church, and P. C. McIntosh, 2014: Seasonal prediction of global sea level anomalies using an ocean–atmosphere dynamical model. *Climate Dyn.*, **43**, 2131–2145, doi:10.1007/s00382-013-2039-7.

Moftakhari, H. R., D. A. Jay, and S. A. Talke, 2016: Estimating river discharge using multiple-tide gauges distributed along a channel. *J. Geophys. Res. Oceans*, **121**, 2078–2097, doi:10.1002/2015JC010983.

Rencher, A. C., and W. F. Christensen, 2012: *Methods of Multivariate Analysis*. 3rd ed. Wiley, 800 pp.

Roberts, C. D., D. Calvert, N. Dunstone, L. Hermanson, M. D. Palmer, and D. Smith, 2016: On the drivers and predictability of seasonal-to-interannual variations in regional sea level. *J. Climate*, **29**, 7565–7585, doi:10.1175/JCLI-D-15-0886.1.

Ryan, H., H. Gibbons, J. W. Hendley II, and P. Stauffer, 2005: El Niño sea-level rise wreaks havoc in California's San Francisco Bay region. USGS. [Available online at http://pubs.usgs.gov/fs/1999/fs175-99/.]

Saha, S., and Coauthors, 2010: The NCEP Climate Forecast System Reanalysis. *Bull. Amer. Meteor. Soc.*, **91**, 1015–1057, doi:10.1175/2010BAMS3001.1.

——, and Coauthors, 2014: The NCEP Climate Forecast System version 2. *J. Climate*, **27**, 2185–2208, doi:10.1175/JCLI-D-12-00823.1.

Stephens, S. A., R. G. Bell, D. Ramsay, and N. Goodhue, 2014: High-water alerts from coinciding high astronomical tide and high mean sea level anomaly in the Pacific Islands region. *J. Atmos. Oceanic Technol.*, **31**, 2829–2843, doi:10.1175/JTECH-D-14-00027.1.

Timmermann, A., S. McGregor, and F.-F. Jin, 2010: Wind effects on past and future regional sea level trends in the southern Indo-Pacific. *J. Climate*, **23**, 4429–4437, doi:10.1175/2010JCLI3519.1.

Webster, P. J., 1995: The annual cycle and the predictability of the tropical coupled ocean–atmosphere system. *Meteor. Atmos. Phys.*, **56**, 33–55, doi:10.1007/BF01022520.

Widlansky, M. J., A. Timmermann, S. McGregor, M. F. Stuecker, and W. Cai, 2014: An interhemispheric tropical sea level seesaw due to El Niño taimasa. *J. Climate*, **27**, 1070–1081, doi:10.1175/JCLI-D-13-00276.1.

——, ——, and W. Cai, 2015: Future extreme sea level seesaws in the tropical Pacific. *Sci. Adv.*, **1**, e1500560, doi:10.1126/sciadv.1500560.

Wyrtki, K., 1984: The slope of sea level along the equator during the 1982/1983 El Niño. *J. Geophys. Res.*, **89**, 10 419–10 424, doi:10.1029/JC089iC06p10419.

Xu, C., X.-D. Shang, and R. X. Huang, 2014: Horizontal eddy energy flux in the world oceans diagnosed from altimetry data. *Sci. Rep.*, **4**, 5316, doi:10.1038/srep05316.

Yin, Y., O. Alves, and P. R. Oke, 2011: An ensemble ocean data assimilation system for seasonal prediction. *Mon. Wea. Rev.*, **139**, 786–808, doi:10.1175/2010MWR3419.1.